FASEB BioAdvances **WILEY**

RESEARCH ARTICLE

Cementum attachment protein-derived peptide induces cementum formation

Lía Hoz Rodríguez[1] | Maricela Santana Vázquez[1] |
Luis Fernando Ramírez González[1] | Gonzalo Montoya Ayala[1] |
Sonia López Letayf[1] | A. Sampath Narayanan[2] | Higinio Arzate[1]

[1]Laboratorio de Biología Periodontal,
Facultad de Odontología, Universidad
Nacional Autónoma de México, Mexico
City, Mexico

[2]Department of Pathology, School of
Medicine, University of Washington,
Seattle, USA

Correspondence
Higinio Arzate, Laboratorio de Biología
Periodontal, Facultad de Odontología,
Universidad Nacional Autónoma de
México, Mexico City, México.
Email: harzate@unam.mx;
liahoz@comunidad.unam.mx

Abstract

A pentapeptide AVIFM (CAP-p5) derived from the carboxy-terminus end of ce-
mentum attachment protein was examined for its role on proliferation, differenti-
ation, and mineralization of human periodontal ligament cells (HPLC), and for its
potential to induce cementum deposition in vivo. CAP-p5 capability to induce hy-
droxyapatite crystal formation on demineralized dentin blocks was characterized
by scanning electron microscopy, µRAMAN, and high-resolution transmission
electron microscopy. The results revealed that CAP-p5 promoted cell prolifera-
tion and cell differentiation and increases alkaline phosphatase activity of HPLC
and mineralization at an optimal concentration of 10 µg/mL. It induced the ex-
pression of cementum molecular markers BSP, CAP, CEMP1, and ALP at the pro-
tein level. In a cell-free system, human demineralized dentin blocks coated with
CAP-p5 induced the deposition of a homogeneous and continuous mineralized
layer, intimately integrated with the underlying dentin indicating new cementum
formation. Physicochemical characterization of this mineral layer showed that
it is composed of hydroxyapatite crystals. Demineralized dentin blocks coated
with CAP-p5 implanted subcutaneously in BALB/cAnNCrl were analyzed histo-
logically; the results disclosed that CAP-p5 could induce the deposition of a ce-
mentum layer intimately integrated with the subjacent dentin with cementocytes

Abbreviations: ACS, absorbable collagen sponge; ADP5, amelogenin-derived peptide 5; ALP, alkaline phosphatase mineralization associated; ARS,
alizarin red S; BGLAP, osteocalcin; BMPs, bone morphogenetic proteins; BSA, bovine serum albumin; BSP, bone sialoprotein; CAP, cementum
attachment protein; CAP-p5, cementum attachment protein-derived peptide-5; CEMP1, cementum protein 1; CEMP1-p1, Cementum Protein
1- derived peptide1; CPC, cetylpyridinium chloride; DFC, dental follicular cells; EDS, energy dispersive spectroscopy; EDTA,
ethylenediaminetetraacetic acid tetrasodium salt dihydrate; EMD, enamel matrix derivative; FBS, fetal bovine serum; FE-SEM, field-emission
scanning electron microscopy; FITC, Fluorescein-5-isothiocyanate; Fmoc, 9-fluorenylmethoxycarbonyl; FN1, Fibronectin; GAPDH, glyceraldehyde-
3-phosphate dehydrogenase; GTR, guided tissue regeneration; HA, hydroxyapatite; HACD1, 3-hydroxyacyl-CoA dehydratase; HPLC, human
periodontal ligament cells; HRP, horseradish peroxidase; HRTEM, high resolution transmission electron microscopy; IGF-I, insulin-like growth
factor I; MEPE, matrix extracellular phosphoglycoprotein; MGP, matrix GLA protein; MSCs, mesenchymal stem cells; MTT, 3-(4,5-dimethylthazol-2-
yl)-2,5-diphenyl tetrazolium bromide; PBS, phosphate buffered saline; PDGF, platelet derived growth factor; PDL, periodontal ligament; PVDF,
polyvinylidene difluoride; SEM, scanning electron microscopy; SPP1, secreted phosphoprotein 1; SPS, simulated physiological solution; TGF-β1,
transforming growth factor beta 1; VTN, Vitronectin.

embedded into the cementum matrix. Immunostaining showed the expression of cementum molecular markers; *v.gr.* BSP, CAP, CEMP1 and ALP, validating the molecular identity of the newly deposited cementum. We conclude that CAP-p5 is a new biomolecule with the potential of therapeutic application to contribute to the regeneration of cementum and periodontal structures lost in periodontal disease.

KEYWORDS

cementum, cementum attachment protein, peptide CAP-p5: Cementum proteins, periodontal regeneration

1 | INTRODUCTION

Cementum is one component of the most complex biological system in mammals: the periodontium. This mineralized connective tissue covers the entire surface of the root and constitutes the interface between the periodontal ligament and dentin. Cementum contributes to the anchorage of the collagen fiber bundles of the periodontal ligament and the supra-alveolar gingival fiber system, providing biomechanical and structural support for the connective tissue attachment; therefore, cementum and the periodontal ligament are intricately connected.[1] Homeostasis of the periodontium is lost when this physiological system is affected by periodontitis, a chronic multifactorial disease, leading to its destruction and tooth loss.[2] Ideally, periodontal therapy has been directed to re-establish the anatomy and a fully functional attachment apparatus of periodontal tissues affected by periodontal disease. These include standard surgical procedures, the use of barrier membranes for guided tissue regeneration (GTR)[3,4] enamel matrix derivative (EMD)[5,6] bone morphogenetic proteins (BMPs),[7] growth factors such as PDGF,[8–10] IGF-I,[11] and TGF-β1superfamily proteins,[12] and multifunctional scaffolds.[13] Lately the combination of MSCs, growth factors, and a scaffold has also been proven to succeed in recreating an osteogenic construct.[14] However, the therapeutical approaches used nowadays have failed to completely restore the anatomy and function of a healthy periodontium, and the results are not predictable. Hence, novel therapeutic strategies that facilitate the regeneration of normally functioning periodontal apparatus in the diseased periodontium are being investigated.

Within the intricacy of the regeneration of the periodontal functional unit, cementum plays a key role to regulate the periodontium microenvironment to achieve the neoformation of periodontal tissues. Cementum extracellular matrix is composed of collagen types I and III,[15] glycoproteins such as osteopontin, also known as secreted phosphoprotein 1 (SPP1),[16] bone sialoprotein (BSP), osteocalcin (BGLAP), matrix GLA protein (MGP), alkaline phosphatase mineralization associated (ALP),[17] fibronectin (FN1) and vitronectin (VTN).[17,18] Cementum also has shown to contain proteins called Cementum Protein 1 (CEMP1)[19] and Cementum Attachment Protein (CAP),[20] these proteins are expressed by cementoblasts and mesenchymal stem cells in the periodontium, and they promote cell attachment and periodontal ligament cells differentiation toward the cementoblastic phenotype. In addition, these proteins are potent regulators of hydroxyapatite crystal nucleation and its growth in vitro.[21–23] These proteins have been shown to promote bone regeneration in criticalsized calvaria defects.[23,24] Cementum Attachment Protein is an isoform and homonym of 3-hydroxyacyl-CoA dehydratase (HACD1).[20] Previous studies have unveiled the role of CAP regulating the mineralization process in vitro and in vivo.[23] Recently, we demonstrated that CAP's carboxylterminus nucleates hydroxyapatite crystals in vitro and induces HPLC differentiation.[25] The CAP's *C-terminus* sequence comprises 15 amino acids, which replaces the active site for HACD1 phosphatase activity. Synthetic peptides are cost-effective small molecules with high regenerative competency, biocompatibility, and straightforwardly synthesized with manageable properties that make them perfect biomolecules with noteworthy impact on tissue regeneration. Therefore, we designed a pentapeptide from the carboxy-terminus sequence of CAP. This peptide with the sequence AVIFM is hereinafter referred to as CAP-p5. We examined the influence of this peptide on cell proliferation, cell differentiation, and mineralization of HPLC. We investigated specific effects of the CAP's-p5 on de novo cementum formation on dentin blocks coated with CAP-p5 and subcutaneously implanted into BALB/cAnNCrl.

2 | MATERIALS AND METHODS

2.1 | Ethics statement

The Ethics Committee at the Facultad de Odontología, of the Universidad Nacional Autónoma de México (UNAM),

reviewed and approved the use of human tissue from the oral cavity for the generation and culturing of HPLC and all animal procedures. Tissue samples were obtained from donors who underwent routine oral surgery procedures.

2.2 | Peptide Synthesis

The pentapeptide sequence corresponds to aminoacids 136 to 140 of the CAP's carboxy-terminal domain: AVIFM. The synthesis of the peptide was performed as described elsewhere.[26] Briefly, the peptide was synthesized by standard Fmoc solid-phase peptide synthesis and purified using C-18 reverse-phase liquid chromatography up to a > 95% purity level (Byosinth, Gardner, MA, USA). Lyophilized CAP-p5 was dissolved in deionized water and the solution filtered (0.22-μm filter) and maintained at 4°C until use.

2.3 | Cell culture

Human periodontal ligament cells (HPLC) were isolated and maintained as previously described.[27] The experimental studies used cells between 2nd and 5th passages. The cells were grown and maintained in DMEM supplemented with 10% fetal bovine serum (FBS; Thermo Fisher Scientific, Waltham, MA, USA), antibiotics (penicillin 100 UI/mL; streptomycin 100 μg/mL) in 5% CO_2 and 95% air atmosphere with 100% humidity.

2.4 | Effect of CAP-p5 on cell proliferation

To evaluate the effect of CAP-p5 on HPLC proliferation, the colorimetric 3-(4,5-dimethylthazol-2-yl)-2,5-diphenyl tetrazolium bromide (MTT) assay was used. HPLC were plated at 0.5×10^4 density in 96-well plates (Thermo Fisher Scientific, Waltham, MA, USA). Experimental cells were treated with CAP-p5 at 1, 5, 10 and 15 μg/mL concentrations in DMEM supplemented with 0.5% FBS for 0, 24, 48, 72, and 96 h. Medium was replaced with fresh CAP-p5 every other day. Control cells did not receive CAP-p5 treatment and were cultured in the presence of 0.5% or 10% FBS, as negative and positive controls, respectively. At the end of each time interval, 10 μL MTT solution (5 mg/mL; Boehringer Mannheim, Indianapolis, IN, USA) in PBS were added to the wells and incubated at 37°C for 4 h. After MTT incubation, 100 μL lysing buffer (20% sodium dodecyl sulfate, 50% dimethyl formamide [pH 4.7]) was added to each well and incubated 1 h at 37°C. Afterward, the resultant solution was read at 570 nm on a microplate reader (Filter Max F5; Molecular Devices, Sunnyvale, CA, USA).

2.5 | Detection and Quantification of Mineralization

Human periodontal ligament cells were plated at a density of 5×10^4 cells, in 6-well plates (Thermo Fisher Scientific, Waltham, MA, USA) and incubated with 10% FBS, 5 mM β-glycerophosphate, and 50 μg/mL ascorbic acid (controls) or with 10 μg/mL of CAP-p5 (experimental) for 5, 10, and 15 days. Cell culture media was replaced every other day and cells were fixed with 70% ethanol and air-dried at various time intervals. Cell cultures were tested for calcium precipitation by staining with 2% Alizarin Red S (ARS; Millipore Sigma, Burlington, MA, USA) for 10 min. To quantify the calcium deposit's staining intensity, the cetylpyridinium chloride (CPC) method was used. Briefly, after staining with ARS, CPC (10%, w/v, in distilled water; Millipore Sigma) was added to each dish (2 mL/dish) and incubated for 1 h at 37°C. After incubation, the transparent CPC solution turned purple, was diluted 5 times (10% w/v) and transferred to a 96-well plate (100 μL/well) for absorbance reading, at 570 nm (Filter Max F5; Molecular Devices). Experiments were performed in triplicate and repeated twice.

2.6 | Alkaline Phosphatase Specific Activity

ALP-specific activity was determined on HPLC (untreated and treated with 10 μg/mL of CAP-p5) and cultured for 5, 10 and 15 days. ALP activity assays were performed as described by Lowry et al.[28] The activity was expressed as nanomoles of p-nitrophenol per minute per milligram of protein and alkaline phosphatase enzymatic activity was normalized to total protein concentration.[29] Data are shown as mean ± S.E.M. from three independent experiments with $p < 0.05$ considered statistically significant. Data were analyzed using Student t test. Statistical analyses were performed with Sigma Stat V 3.1 software (Systat, San Jose CA, USA).

2.7 | Western blot analysis

Human periodontal ligament cells were plated at 2×10^4 density in 6-well culture plates and cultured for 5, 10, and 15 days, treated with or without 5 μg/mL CAP-p5. At the end of the experimental period, the cells were scraped with a policeman and dissolved in lysis buffer containing 1% SDS and protease inhibitor cocktail. Western blots were performed with rabbit polyclonal antibodies anti-human recombinant CAP (produced in house), anti-human recombinant CEMP1 (produced in house), anti-human GAPDH (sc-13,179; Santa

Cruz Biotechnology, Dallas, TX, USA), monoclonal antibody anti-human BSP (sc-73,497; Santa Cruz Biotechnology, Dallas, TX, USA) and monoclonal antibody anti-human ALP (sc-365,765; Santa Cruz Biotechnology, Dallas, TX, USA). Proteins from experimental and control groups (20 μg/lane) were separated on SDS/12% PAGE and electroblotted on a PVDF membrane (Immobilon-P; Millipore Sigma). Membranes were blocked with 5% nonfat milk for 1 h and then incubated with 1:1000 diluted antibodies for 1 h. After they were washed, the membranes were incubated with 1:1000 diluted Goat anti-Rabbit IgG (H+L) secondary antibody, HRP (31,460; Thermo Fisher Scientific, Waltham, MA, USA), or Goat anti-Mouse IgG (H+L) secondary antibody, HRP (31,430; Thermo Fisher Scientific, Waltham, MA, USA) for 1 h. Membranes were washed with PBS and developed as described elsewhere.[19] For assessment of the Western blot, all membranes were digitalized with an Epson V550 scanner and processed and analyzed with ImageJ software National Institutes of Health (NIH), Bethesda, MD, USA. The relative level of each protein was assessed by measuring the integrated intensity of all pixels in each band, excluding the local background. Results are expressed as percentages of protein intensity.

2.8 | Deposition of Hydroxyapatite Crystals on Dentin Blocks Induced by CAP-p5

Human teeth were gathered at the Facultad de Odontología, Universidad Nacional Autónoma de México. The use of these materials complied with the Institutional Review Board Guidelines (approved protocol: CIE: CIE/0101/10/2023). Dentin blocks were prepared as follows: teeth, were extensively washed with PBS, and the remaining soft tissue was detached with a 7/8 Gracey curette. Then, under a stereoscopic microscope the cementum layer was scrapped with a 30/33 Jaquette Scaler until the cementum was completely scraped. Dentin blocks specimens (3 × 3 mm; 1,5 mm thick) were prepared with a diamond disk under copious irrigation, then the blocks were sonicated for 10 min to eliminate tissue debris. Dentin blocks were extensively washed in deionized water and demineralized with 38% phosphoric acid gel for 45 s and extensively washed with deionized water. The specimens were stored in 70% ethanol at 4°C until used. Dentin blocks were coated with 50 μg of CAP-p5 solution dropped on top and vacuum dried. Control dentin blocks were dropping 25 μL of deionized water (23). The specimens were then submerged in a simulated physiological solution SPS; 1.2 mM $CaCl_2 \cdot 2H_2O$, 50 mM HEPES buffer,

0.72 mM KH_2PO_4, 16 mM KCl, 4.5 mM NH_4Cl, 0.2 mM $MgCI_2 \cdot 6H_2O$, pH = 7.15 and incubated for 7 days at 37°C.[30]

2.9 | Characterization of the Mineral Deposits on Dentin Blocks

2.9.1 | Scanning Electron Microscopy

After 7 days of incubation, the morphology, microstructure, and the elemental chemical composition of the precipitates formed on the dentin blocks (coated with CAP-p5 or uncoated), were examined with the JSM-7800F Schottky FE-SEM. The dentin blocks were fixed in an aluminum specimen holder and the samples weas sputter-coated in gold (3 nm) to reduce charge. The images were obtained with backscattered electron signal (BSE). The calcium to phosphate (Ca/P) ratio was calculated from the semi-quantitative analysis obtained by EDS pattern at 20–25 V acceleration voltage and at 20–25 Pa of pressure in the specimen chamber on different areas with different probe sizes (Noran X-ray microanalysis detector, model Voyager 4.2.3.).

2.9.2 | μRaman

Spectra from crystals precipitated on dentin blocks (with and without CAP-p5 treatment) were recorded with a Micro-Raman (Thermo Fisher Scientific, Waltham, MA, USA) with an excitation source of 532 nm, power of 8 mW, and 50–3000 cm-1. A 50 objective with a numerical aperture of 0.75 was used to focus the sample and collect the spectra for 12 s. Samples were positioned horizontally on a plastic specimen holder, and a region of interest was selected using an integrated optical microscope. The vibratory spectra from functional groups were analyzed with the Origin Pro 2020 software (OriginLab, Northampton, MA, USA).

2.9.3 | High resolution transmission electron microscopy (HRTEM)

The calcium phosphate precipitates obtained from dentin blocks (with and without CAP-p5 treatment) were suspended in isopropyl alcohol and dispersed by ultrasonic bath, then a drop was placed on carbon Formvar-coated copper grids of 300 mesh. The samples were characterized by transmission electron microscopy (JEOL JEM-2010F FasTEM microscope) operated at 200 kV. Digital Micrograph software was used to analyze the crystal structure of the samples. The interplanar distances were

compared to standard hydroxyapatite (JCPDS 72–1243) and monetite (JCPDS 03–0398).

2.9.4 │ Resin infiltration and backscattered scanning electron microscopy

For backscattered scanning electron microscopy (SEM), the surfaces of the methyl methacrylate-embedded dentin blocks were polished. The specimens were examined with JSM-7800F Schottky FE-SEM microscope.

2.9.5 │ In Vivo Subcutaneous Implantation of Dentin Blocks coated with CAP-p5

The Protocols used in these studies were approved by the Institutional Animal Care and Use Committee at the School of Dentistry, Universidad Nacional Autonoma de Mexico (approved protocol FO-M001-0009-2022). Five male BALB/cAnNCrl aged 2 months and weighing 25–30 grams were obtained from the Instituto de Fisiología Celular, Vivarium. The animals were acclimatized for 7–14 days at a temperature 18–22°C and relative humidity 30%–70% with a 12/12 h light/dark cycle. The animals had ad libitum access to water and a standard laboratory diet. The same animal served as control and experimental. Dentin blocks dimensions were: 3×3 mm; 1,5 mm thick. (1). Control group: On the right site of the male BALB/cAnNCrl mice dorsum were implanted the dentin blocks treated with deionized water. (2). Experimental group. On the left side of the male BALB/cAnNCrl dorsum dentin blocks treated with 50 µg of CAP-p5 were implanted, (see Figure 1). Dentin blocks specimens from both groups (control and experimental) were vacuum dried prior to the subcutaneous implantation. A surgical subcutaneous incision was performed in male BALB/cAnNCrl, anesthetized by intraperitoneal injection of 80 mg/kg ketamine and 10 mg/kg xylazine. A 1 cm incision was performed at the center of the dorsum. The control and experimental dentin blocks specimens were placed subcutaneously, and skin was sutured with 5–0 Vicryl™ absorbable sutures (Ethicon Inc., Bridgewater, NY, USA). The procedures were performed under aseptic conditions. After 16 weeks, animals were euthanized using carbon dioxide gas USP Grade A.

2.9.6 │ Histologic Procedures

Immediately after the euthanasia, dentin blocks were recovered and fixed in 10% formaldehyde for 5 days. The dentin blocks were decalcified with 10% EDTA
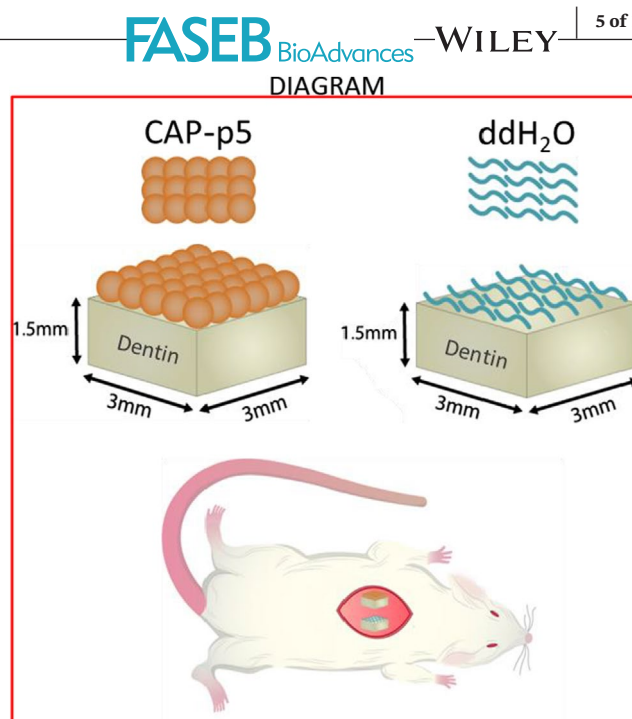
DIAGRAM

FIGURE 1 CAP-p5 dentin blocks coating and subcutaneous implantation in BALB/cAnNCrl mice.

(pH 7.4), containing 0.5% formaldehyde for 30 days, dehydrated in a graded alcohol series, embedded in paraffin. Sections 5 mm thick were cut and mounted on glass silanized slides, as described elsewhere.[23] Panoramic photomontages acquired from three central sections per defect and stained with hematoxylin and eosin were used for histological and histomorphometric analyses to assess the formation of new cementum on dentin blocks treated with CAP-p5. Three sections were stained with Masson's trichrome stain for cross-reference. The sections were examined via light microscopic analysis (Axioskope 2; Zeiss, Germany) and performed by two-blinded examinators.

2.9.7 │ Immunofluorescence

Expression of cementum-related molecular markers were analyzed in the dentin blocks with and without CAP-p5 treatment by double-immunofluorescence staining using the following antibodies: 1. Rabbit anti-human recombinant CAP polyclonal antibody (produced in house), diluted 1:100; rabbit anti-human recombinant CEMP1 (produced in house), diluted 1:50; 3. rabbit anti-human ALP (PA5-8335; Thermo Fisher Scientific, Waltham, MA, USA), diluted 1:50 and 4: mouse anti-human BSP (SC-73497; Santa Cruz Biotech., Inc. Dallas, Texas, USA) diluted 1:100. Antibodies were diluted in PBS containing 2 mg/mL of BSA to block unspecific binding of the antibody. Sections were incubated with primary antibodies as described above and incubated overnight at 4°C. Sections were washed with PBS containing 0.1% Tween 20,
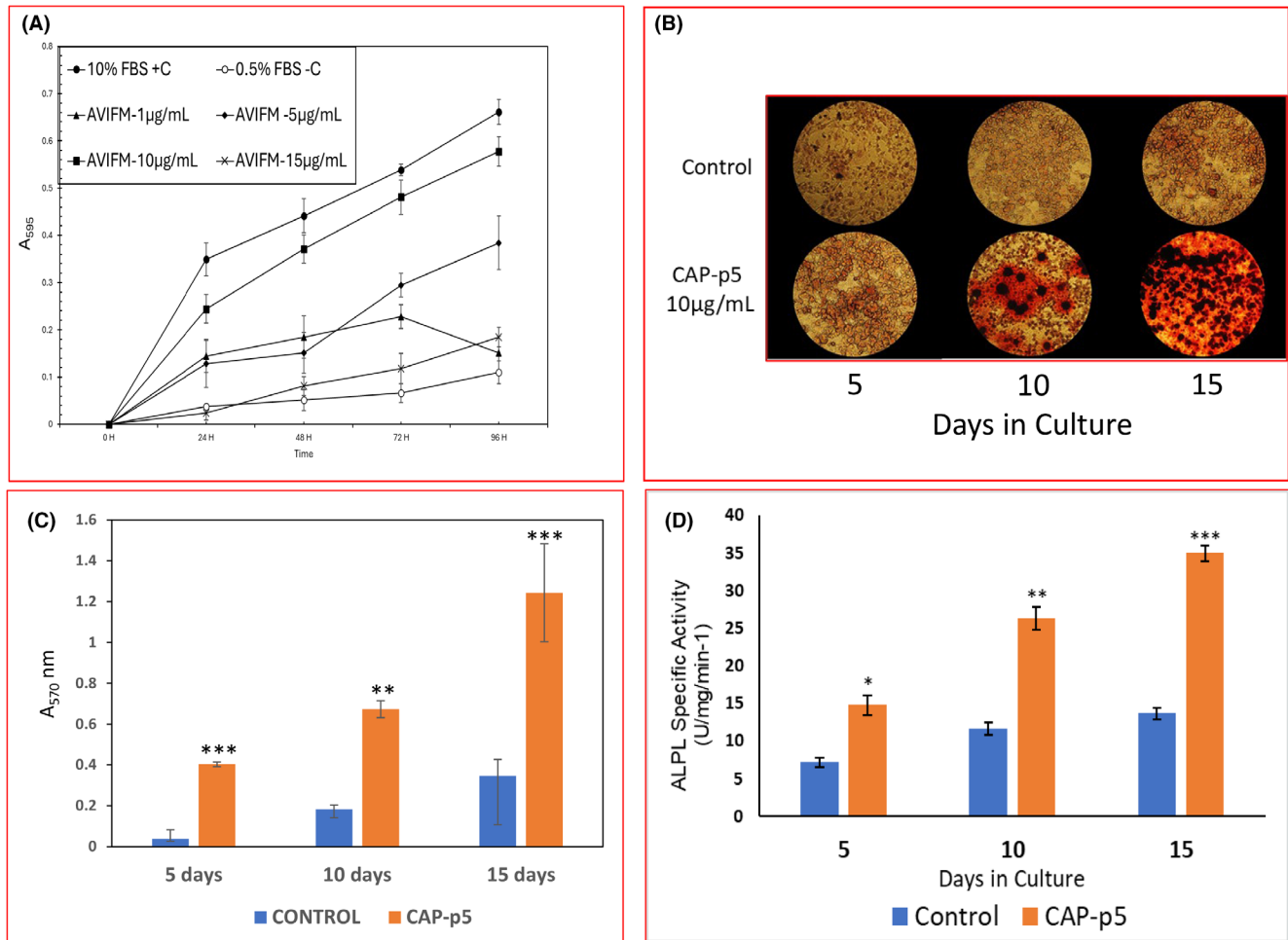
FIGURE 2 (A) Synthetic Cementum Attachment Protein-Derived Peptide (CAP-p5) stimulated HPLC proliferation with an optimal concentration of 10 μg/mL by 71, 84, 89 and 86% at 1, 2, 3, and 4 days, respectively. (B) Representative images of HPLC after osteogenic induction elicited by CAP-p5 at 10 μg/mL of cultures stained with 2% solution of ARS at 5, 10, and 15 days, (C) Elution of ARS with Cetylpyridinium Chloride showed that the calcium contents of HPLC treated with CAP-p5 at 10 μg/mL concentration are significantly higher than those of the control cells. (D) Alkaline phosphatase specific activity was increased by HPLC treated with CAP-p5 at 10 μg/mL concentration at 5, 10, and 15 days. All assays were repeated three times independently ($n = 3$/group). *$p < 0.05$, **$p < 0.01$, and ***$p < 0.005$.

three times for 5 min, then with PBS for 5 min. Sections were then incubated with 1:400 diluted (in PBS), goat anti-mouse IgG (H+L) highly cross-adsorbed secondary antibody, Alexa Fluor™ Plus 488 (A32723; Thermo Fisher Scientific, Waltham, MA, USA) and goat anti-rabbit IgG (H+L) cross-adsorbed secondary antibody, Alexa Fluor™ 594 (A-11012; Thermo Fisher Scientific, Waltham, MA, USA) for 1 h at room temperature. The samples were evaluated with a fluorescence microscope (Axioskope 2; Zeiss, Germany), with the appropriate filter combinations. Negative controls were achieved by omitting the primary antibody or by incubating with normal mouse or rabbit serum.

2.10 | Statistical analysis

Unpaired Student t tests were used to compare the control groups against the experimental group at 4 weeks

post-surgery. All results are expressed as mean ± SE, and a value of $p = 0.05$ was considered statistically significant. Statistical analyses were performed with Sigma Stat V 3.1 software (Systat, San Jose CA, USA).

3 | RESULTS

3.1 | Cell proliferation

The results showed that CAP-p5 optimally stimulated HPLC proliferation at a 10 μg/mL concentration. The stimulation was 71, 84, 89 and 86% at 1, 2, 3, and 4 days respectively, when compared to the positive control (10% FBS; Figure 2A).

CAP-p5 Induced HPLC toward a Mineralizing Phenotype.

Human periodontal ligament cells were treated with CAP-p5 (10 μg/mL) and assessed for mineral production

with ARS. The results revealed the formation of calcium nodules by HPLC treated with CAP-p5. Control cultures did not form calcium nodules (Figure 2B). Quantification of staining using CPC demonstrated significant differences of staining intensity between CAP-p5-treated HPLC cultures by 10.0, 3.7 and 5.2-fold at 5, 10 and 15 days, when compared to controls (Figure 2C).

Alkaline Phosphatase Specific Activity of HPLC treated with 10 μg/mL of CAP-p5 at 5, 10 and 15 days revealed that ALP-specific activity raised by 2.1, 2.3 and 2.6-fold, respectively, when compared to untreated controls. (Figure 2D).

3.2 | Expression of Cementum-Associated Proteins by Human Periodontal Ligament Cells

The differentiation effect of CAP-p5 on HPLC toward cementoblast-like cell phenotype was assessed at the protein level by Western blot analysis (Figure 3A). The expression of cementum-related molecules was assessed at 5, 10, and 15 days. The results revealed that treatment of HPLC cultures with CAP-p5 (10 μg/mL), increased the expression of ALP by 83, 80, and 138% HPLC cultures treated with CAP-p5 at 5, 10, and 15 days, when compared to the controls (Figure 3B). BSP was expressed by 39% both at 10 and 15 days in experimental cultures, when compared to controls respectively. Cell cultures treated with CAP-p5 revealed a positive effect on the expression of CAP by 64.6, 123, and 107% when compared with control cultures at 5, 10, and 15 days respectively. Cementum Protein 1 expression by HPLC treated with CAP-p5 increased by, 129, 95 and 89% at 5, 10 and 15 days of culture respectively, relative to controls.

3.3 | Analyses of Mineral Deposits on Dentin Blocks

3.3.1 | Scanning Electron Microscopy and μRaman Spectroscopy

SEM analysis of the mineral deposits on control dentin blocks revealed crystal features of flake-like crystals, with almost parallel and linear organization (Figure 4A). Dentin blocks coated with CAP-p5 promoted the formation of lamellae-like crystal structures, with irradiating plate-like crystals emerging out of the underlying dentin surface. (Figure 4B). Further confirmation of the nature and structural changes of the crystals deposited on dentin blocks treated with CAP-p5 and controls was performed using μRaman spectroscopy. A representative μRaman spectrum of control and CAP-p5 samples
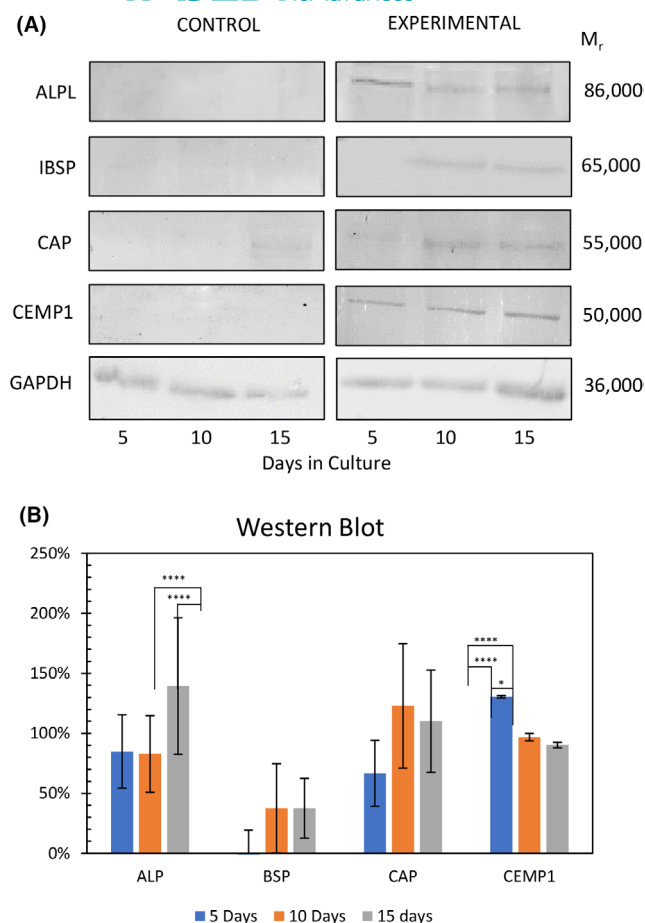
FIGURE 3 (A) Human periodontal ligament cells cultured without CAP-p5 showed practically undetectable expression at the protein level of ALP and CEMP1. However, CAP was expressed at 15 days of culture. Human periodontal ligament cells treated with CAP-p5 at 10 μg/mL concentration revealed a noteworthy gene product expression of ALP, CAP, and CEMP1 at 5, 10, and 15 days of culture. Nevertheless, BSP was noticeably expressed at 10 and 15 days of culture. (B) Cementum-related molecules expression when compared to controls. $*p < 0.05$; $****p < 0.0001$.

are shown (Figure 4C). Micro-Raman bands for controls showed the most intense band at 987 cm^{-1} corresponding to symmetric PO stretching (v_1). Raman spectra of CAP-p5 showed the most intense band at 963 cm^{-1} due to the symmetric stretching mode of the P–O bond $v_1(PO_4)$. The results show that spectra assigned to the control and CAP-p5 phase are visibly distinguishable. We observed the distinct shifts and splitting of the HPO_4^{2-} vibrational frequencies in the control spectra with the normal modes of the isolated phosphate ion PO_4^{3-} observed in CAP-p5 due the presence of hydroxyapatite. EDS elemental analysis was carried out to measure the calcium to phosphorus (Ca/P) molar ratio of the samples. Mineral deposits on dentin blocks coated with CAP-p5 after incubation for 7 days in SPS had a Ca/P molar ratio of 1.57 ± 0.07 (inset), which is close to the theoretical
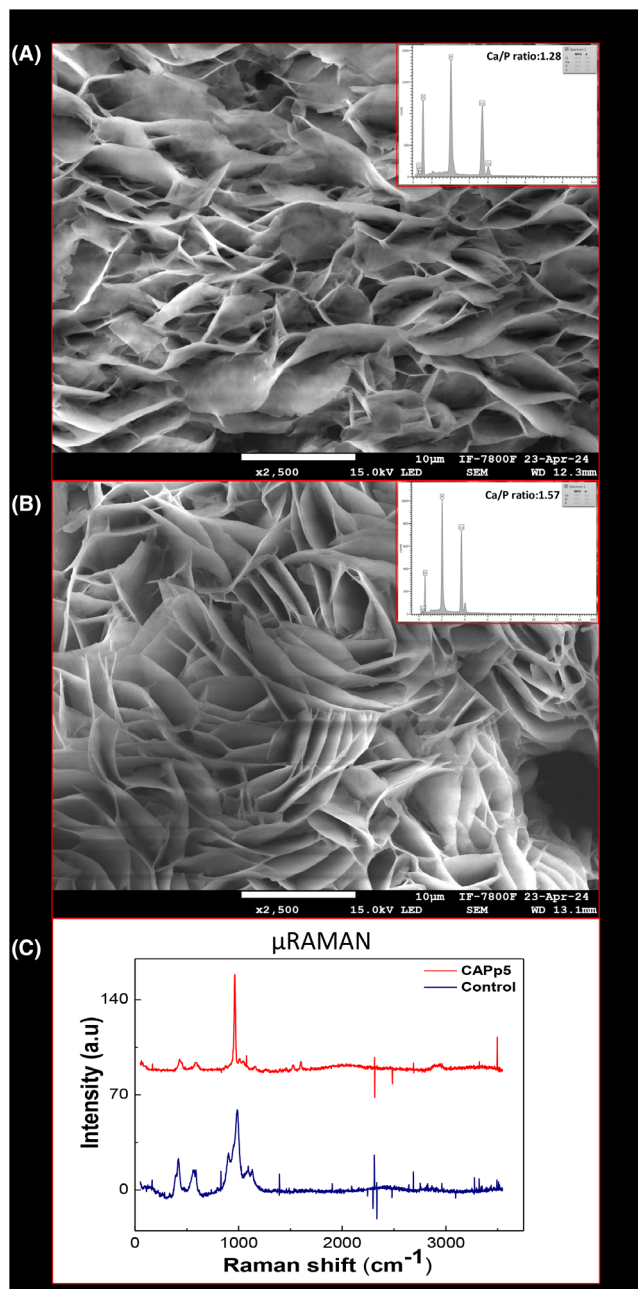
FIGURE 4 (A) SEM images of the mineral deposits on control dentin blocks revealed features of flake-like crystals, with almost parallel and linear organization with a CA/P ratio: 1.28 (inset). (B) Dentin blocks coated with CAP-p5 promoted the formation of lamellae-like crystal structures, with irradiating plate-like crystals emerging out of the underlying dentin surface with a Ca/P ratio: 1.57 (inset), representing hydroxyapatite. (C) Further confirmation of the nature and structural changes of the crystals deposited on dentin blocks treated with CAP-p5 and controls was performed using μRaman spectroscopy.

value of stoichiometric hydroxyapatite (inset). Controls had a Ca/P molar ratio of 1.28 ± 0.03 (inset).

Control and experimental samples embedded in resin showed distinct differences in the remineralization of dentin blocks as observed by SEM. After 7 days of dentin blocks
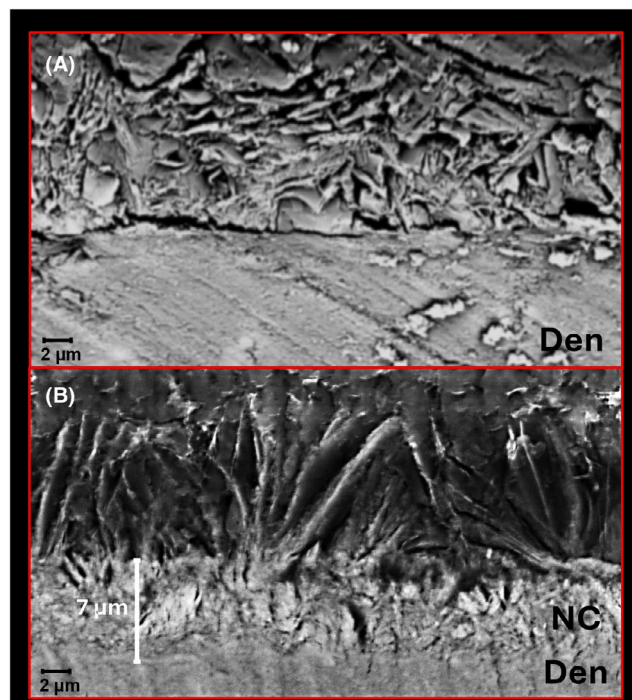

FIGURE 5 SEM images of resin embedded samples. (A) Lateral view of controls samples without CAP-p5 treatment revealed a disorganized crystals and a gap between crystal layer and the underlying dentin surface. (B) Dentin blocks treated with CAP-p5 displayed a homogeneous and uniform thickness of cementum-like layer firmly integrated to the subjacent dentin. Den, dentin, NC, new cementum.

incubation in SPS, a disorganized layer of crystallites with a gap between the underlaying dentin and crystals was observed in control samples without the peptide Figure 5A. However, a newly, homogeneous, and continuous layer of mineral with an intimate union with the surface of the underlying dentin was observed in specimens coated with CAP-p5 (Figure 5B). The morphological features revealed that the layer was composed of globular material with a thickness of 7 μm comprising biomimetic cementum in an in vitro system, that continued to form needle-like crystals.

3.3.2 | High-Resolution Transmission Electron Microscopy (HRTEM)

HRTEM provided further insight into the nanometer-scale details of the samples. The HRTEM images and corresponding fast Fourier transform (FFT) revealed the single-crystal nature of monetite according to JCPDS 03–0398 in the control sample (Figure 6A). The interplanar distances measured in segments of the HRTEM micrograph were 0.447 and 0.426 nm, corresponding to the interplanar spacing of the (011) and (101) crystal planes of monetite. For the crystals induced by CAP-p5, the diffraction spots were assigned as a single crystal diffraction
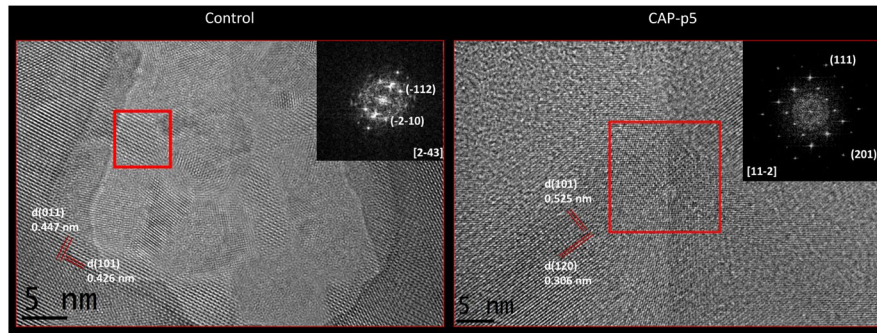
FIGURE 6 (A) The HRTEM images and corresponding fast Fourier transform (FFT) revealed the single-crystal nature of monetite according to JCPDS 03–0398 in the control sample. The interplanar distances were 0.447 and 0.426 nm, corresponding to the interplanar spacing of the (011) and (101) crystal planes of monetite. (B) For the crystals induced by CAP-p5, the diffraction spots were assigned as a single crystal diffraction of hydroxyapatite taken along the [11-2] direction. The interplanar distances were 0.525 nm and 0.306 nm corresponding to the planes (101) and (120) for hydroxyapatite according to JCPDS 72–1243.
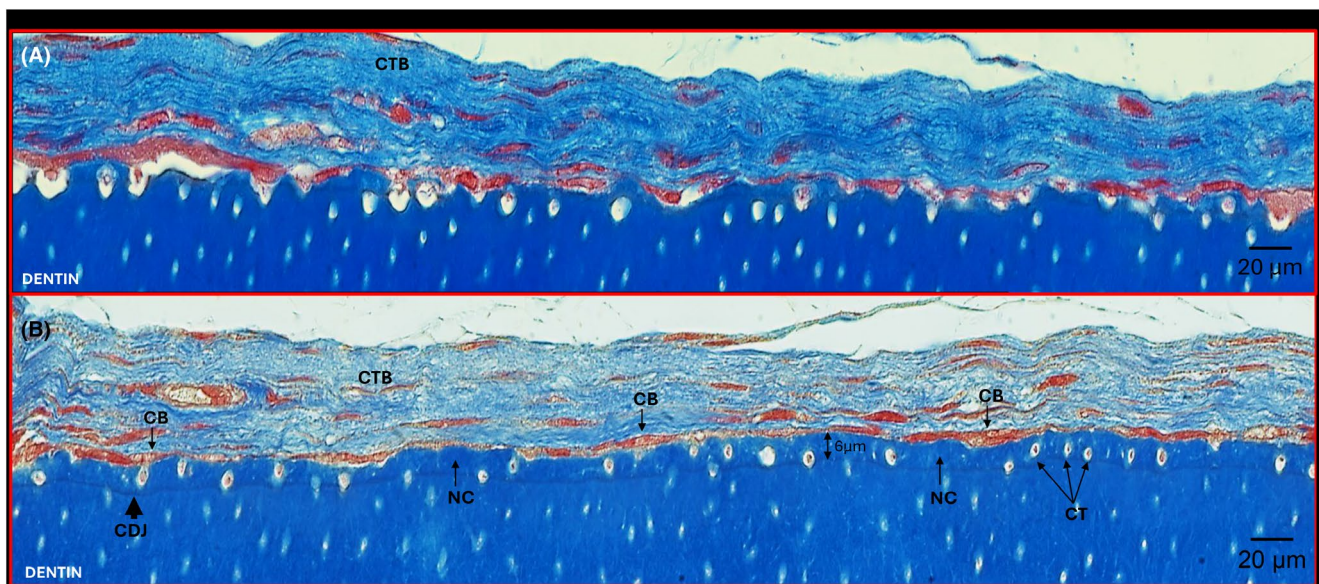
FIGURE 7 Dentin block with and without CAP-p5 coating implanted in the dorsum of BALB/cAnNCrl and left in situ for 16 weeks. (A) Histologic sections were stained with Masson's trichrome. Control dentin implants (without CAP-p5 coating) exhibited connective fibrous tissue layer without evidence of cementum deposition on the underlying dentin. (B) Dentin blocks coated with CAP-p5 implanted subcutaneously in BALB/cAnNCrl revealed dense fibrous connective tissue with putative cementoblast bordering a well-defined continuous layer of new cementum firmly integrated with the underlaying dentin. CB, cementoblast; CDJ, cementum-dentin junction; CT, cementocyte; CTB, Connective tissue bundles; NC, new cementum.

of hydroxyapatite taken along the [11-2] direction. The interplanar distances were 0.525 nm and 0.306 nm corresponding to the planes (101) and (120) for hydroxyapatite according to JCPDS 72–1243 (Figure 6B).

3.3.3 | Histological analysis for Cementum formation induced by CAP-p5 in BALB/cAnNCrl

To determine whether CAP-p5 can induce cementum formation on CAP-p5-coated dentin blocks, we used a BALB/cAnNCrl mouse model. After 16 weeks of subcutaneous implantation control dentin blocks were covered by dense fibrous connective tissue bundles, cells were aligned and facing the irregular dentin surface. Notably, there was no evidence that the cells facing the dentin surface deposited mineralized material on dentin blocks (Figure 7A). Dentin blocks coated with CAP-p5 revealed the formation of densely packed connective fibrous tissue on top of the dentin blocks treated with CAP-p5. The connective tissue contained immersed cells into the fibrous matrix bundles oriented parallelly to the dentin block surface. Cells contained in this matrix were aligned to the

dentin surface and facing the newly formed cementum-like tissue (Figure 7B). The newly deposited cementum-like tissue showed a homogeneous thickness. A consistent line with basophilic affinity staining was observed at the intimate junction between newly deposited cementum and underlying dentin. This newly formed cementum-like tissue showed both cells becoming embedded into the cementoid matrix and cementoblasts trapped into the thickness of newly formed cementum (cementocytes) (Figure 7B). The thickness of new formed cementum was $6.2 \pm 0.04 \mu m$.

3.3.4 | Immunofluorescence

We examined the co-expression of cementum-related proteins BSP with CEMP1, CAP, and ALP by double labeling immunofluorescence. Results showed the molecular composition of the newly formed cementum in the histologic sections. BSP showed strong staining in cells embedded into the collagen fiber bundles of connective tissue covering the dentin implant. Also, moderate staining in the newly deposited cementum was observed. CAP was strongly expressed by cells immersed into the fiber bundles of the connective tissue covering the implant and those resembling putative cementoblasts. Less pronounced staining was observed in the newly formed cementum and colocalization of these molecules was strongly expressed by cells immersed into the extracellular matrix of connective tissue covering the dentin implant. CEMP 1 was strongly expressed by cells covering the newly deposited cementum and cementocytes embedded into the mineralized matrix. BSP and CEMP1 colocalized in cells facing the new deposited cementum (Figure 8). ALP strongly colocalized with BSP in the mineralized matrix of newly formed cementum and in a few cells immersed in the collagen fiber bundles covering the dentin implant (Figure 8). These results demonstrated that CAP, CEMP1 and ALP colocalized with BSP in the mineralized matrix of newly formed cementum and cells representing putative cementoblasts. Controls using pre-immune mouse or rabbit serum were negative (Figure S1).

4 | DISCUSSION

The objective of the present study was to evaluate the biological effect of a cementum attachment protein-derived peptide (CAP-p5) on the differentiation HPLC toward a cementoblast-like phenotype in vitro and on the formation of mineralized layer resembling cementum in vivo. Our study demonstrates that CAP-p5 induces hydroxyapatite crystal nucleation and its regenerative capacity is evidenced by de novo cementum formation on demineralized dentin blocks in vivo. CAP-p5 triggered cell proliferation by HPLC similar to 10% FBS. The most notable effect was observed with an optimal concentration at $10 \mu g/mL$, consequently, the *C-terminal* of cementum attachment protein derived 5-amino acid long peptide (CAP-p5) is a potent regulator of cell growth. Therefore, we infer that CAP-p5 acts as peptide signaling molecule. Our study revealed that CAP-p5 regulates other critical cellular functions such as control of cell differentiation. Human periodontal ligament cells treatment with CAP-p5 had profound effect on HPLC to display a mineralizing-like phenotype, as confirmed by insoluble calcium nodules formation by 10.0, 3.7 and 5.2-fold at 5, 10, and 15 days when compared to controls. This differentiation effect by CAP-p5 was corroborated by ALP specific activity. ALP plays a role during cementum matrix mineralization formation and has been shown to promote the deposition of acellular afibrillar cementum in vivo,[31] and highest ALP activity has been found in periodontal ligament areas related to mineralization, bordering cellular cementum formation.[17] Furthermore, at the protein level, CAP-p5 treatment of HPLC induces a prominent expression of cementum-associated molecules CEMP1 and CAP. These cementum proteins have been shown to be potent regulators of several cell functions in vitro, such as cell attachment, proliferation, and differentiation toward a cementoblastic-like phenotype by HPLC and play an influential role in development and arrangement of calcium phosphate minerals.[32] Their osteoinductive potential to induce bone formation de novo has been shown in critical-size defects in rat calvaria. BSP, an acidic glycoprotein involved in the nucleation of hydroxyapatite crystals in mineralized tissues,[33–36] plays a role during the process of cementogenesis, promoting cell attachment and differentiation of HPLC toward a cementoblastic phenotype. Our results indicate that BSP expression was upregulated by CAP-p5 on HPLC at the early at late stages of mineralization. ALP is highly expressed at the protein level during mineralization, indicating that CAP-p5 triggers ALP expression which correlates its function to the mineralization and deposition of cementum in vivo.

The findings of this study revealed that CAP-p5 allows hydroxyapatite crystal nucleation and growth on demineralized dentin blocks. The EDS compositional analysis disclosed a 1.57 ± 0.07 Ca/P Ratio, representing a calcium-deficient hydroxyapatite which permits crystal solubility, greater bioactivity, and degradability, promoting cell proliferation, ALP activity and strong
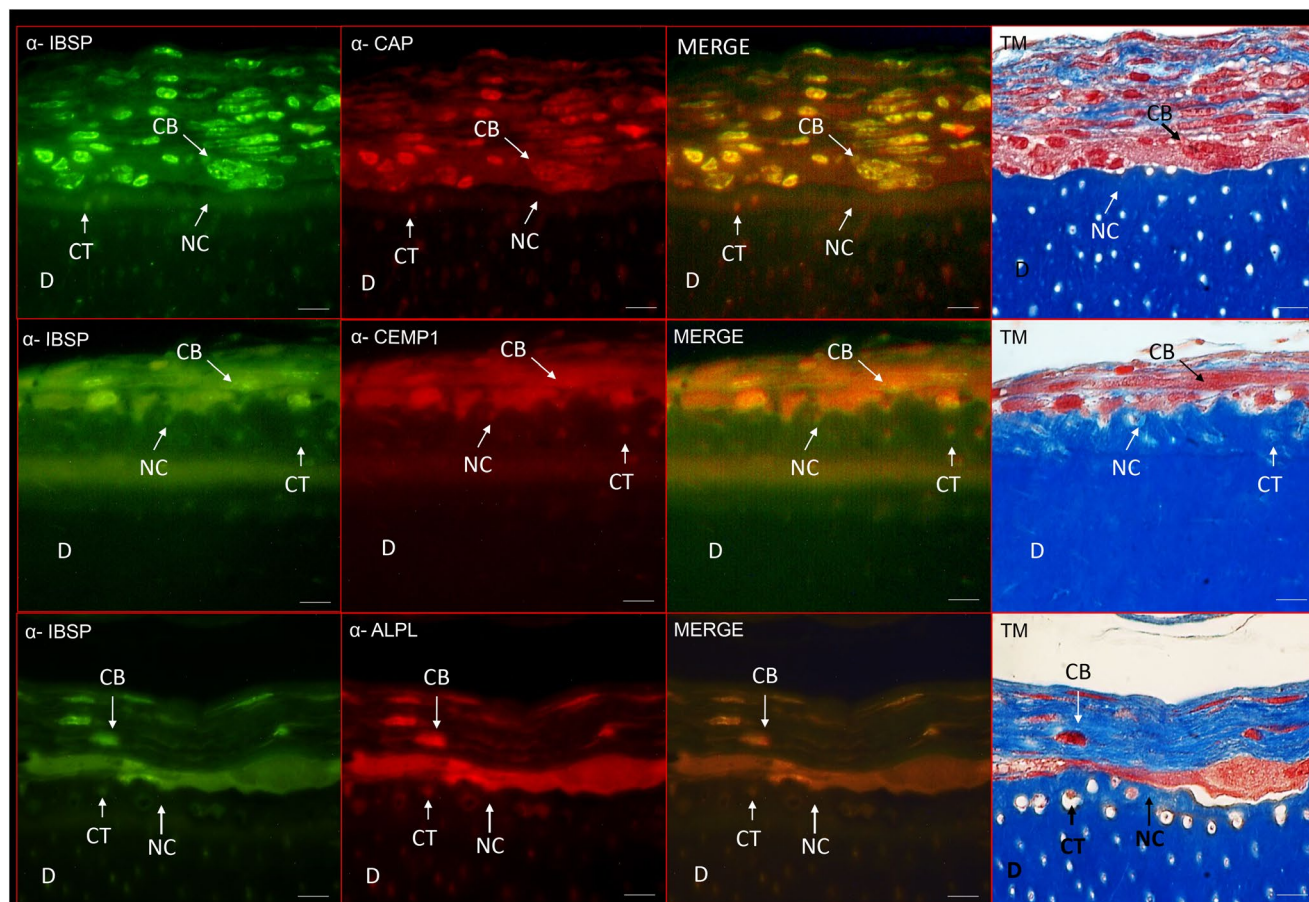
FIGURE 8 Colocalization and double staining of cementum-related molecules (BSP, CAP, CEMP1, ALP) in dentin blocks coated with CAP-p5 and implanted subcutaneously in BALB/cAnNCrl for 16 weeks. BSP localizes on the cells representing putative cementoblasts and the matrix of newly formed cementum. CAP was strongly expressed by cells bordering the newly formed cementum and cementocytes. CEMP1 was localized to the cells and connective tissue matrix covering the underlying newly formed cementum and cementocytes. ALP was strongly expressed in the newly formed cementum mineralized layer and a few cells in the dense connective tissue covering the dentin surface. CAP and CEMP1 were not expressed in the mineralized matrix of the newly formed cementum. Masson's trichromic stain for anatomical orientation. CB, cementoblast; CT, cementocyte; D, dentin; NC, new cementum; TM, Masson's trichomic stain.

expression of osteogenesis-related genes.[37] Moreover, ultrastructural and crystallographic analysis of the crystals formed on dentin blocks coated with CAP-p5, showed that the crystals show lattices and interatomic distances corresponding to hydroxyapatite. Raman spectra of crystals showed the most intense band at 963 cm^{-1} due to the presence of hydroxyapatite. These findings indicate that CAP-p5 has the functional biological activity in terms of hydroxyapatite crystal nucleation as those showed by full-length hrCAP.[23]

Subcutaneous implantation of dentin blocks coated with CAP-p5-coated revealed that in vivo CAP-p5 possesses therapeutic potential to induce cell differentiation and deposition of a mineralized layer of tissues on top of dentin block, which was integrated intimately with the underlying dentin. The characteristics of the deposited layer of tissue show cells embedded into the mineralized matrix. Notably, there is a basophilic strongly stained

material between dentin and the newly deposited mineralized layer. Taken together, these features indicate that this deposited mineralized layer represents cellular cementum, implying that CAP-p5 has the biological properties to induce cell differentiation toward a cementoblast phenotype. Our conclusion is supported by the expression of cementum-related molecules: *v.gr.* BSP, ALP and cementum proteins; CEMP1 and CAP, both in cells representing cementoblasts and in the mineralized matrix of the new cementum. Our results show good biocompatibility in vivo after 4 months of surgical implantation of dentin blocks coated with CAP-p5, enhancing the deposition of new cementum without adverse reactions from the host tissue. Previously several peptides have been shown to have potential to enhance periodontal regeneration, including a self-assembling P$_{11}$-4 peptide,[38] amelogenin-derived peptide 5 (ADP5). The latter mediates periodontal ligament cell proliferation

and attachment on demineralized human dentin and induces the formation of cementum-like mineralized hydroxyapatite layer in a cell-free system.[39] BMP-6/ACS peptide was also shown to be effective for the regeneration of periodontium. In particular, the neoformation of cementum with functionally oriented Sharpey fibers onto critical-size supra-alveolar defects enhanced periodontal wound healing/regeneration, cementogenesis including a functionally oriented periodontal ligament in supra-alveolar periodontal defects in beagle dogs.[40] Synthetic cell binding peptide P-15 in combination with a natural anorganic bovine-derived hydroxyapatite matrix promotes in humans the formation of new cementum, PDL, and alveolar bone on a previously contaminated root surface.[41] A synthetic anabolic peptide (AP) derived from Matrix extracellular phosphoglycoprotein (MEPE) stimulated periodontal regeneration and cementum formation in non-human primate model.[42]

Recently a Cementum Protein 1 derived-peptide (CEMP1-p1) was shown to possess high affinity to hydroxyapatite (HA) crystals and to regulate the cementogenesis at the molecular level. This was demonstrated in vitro using dental follicular cells (DFC), by the increased expression of osteoprogenitor cell markers promoting their growth[43] and cementogenesis and osteogenesis with functional oriented PDL fibers in rat cementum fenestration defects.[44]

From the results revealed by this study, we conclude that CAP-p5 synthetic peptide has potential to induce HPLC differentiation toward a mineralizing-like phenotype through the stimulation of the expression of cementum molecular markers, promotion of nucleation of crystals with the physico–chemical characteristics of hydroxyapatite, and deposition of mineralized tissue with the histological and molecular characteristics of cellular cementum on demineralized dentin slices implanted subcutaneously in BALB/cAnNCrl. This work demonstrates cementum deposition on artificially demineralized human dentin through CAP-p5 peptide-guided remineralization, ultimately forming hydroxyapatite layers constructing a structurally strong interface with the subjacent dentin in vitro and in vivo. We believe that CAP-p5 is a new molecular factor capable of promoting the regeneration of the periodontium lost due periodontal disease and providing new insights for the foundation of CAP-p5 clinical application.

AUTHOR CONTRIBUTIONS

H. Arzate identified the pentapeptide, L. Hoz-Rodríguez M. Santana-Vázquez, L. F. Ramírez-González, G. Montoya-Ayala, and S. López-Letayf, performed the in vitro and in vivo experiments, physico–chemical characterization of the cementum-like tissue in vitro and analyzed the data. L. Hoz-Rodríguez, A. S. Narayanan, and H. Arzate conceived and designed the experiments and wrote the manuscript.

DISCLOSURES

The authors declare no conflicts of interest.

DATA AVAILABILITY STATEMENT

All data obtained in this research are described in the manuscript.

ORCID

Lía Hoz Rodríguez https://orcid.org/0000-0002-8284-0745
Maricela Santana Vázquez https://orcid.org/0000-0001-8810-9091
Luis Fernando Ramírez González https://orcid.org/0009-0001-3383-7873
Gonzalo Montoya Ayala https://orcid.org/0000-0001-9376-7347
Sonia López Letayf https://orcid.org/0000-0001-8447-6425
Higinio Arzate https://orcid.org/0000-0002-3735-4924

REFERENCES

1. Goldberg M. The periodontal ligament-a link between the cementum and alveolar bone. *J Clin Med Res*. 2022;3(1):1-18. doi:10.46889/JCMR.2022.3106
2. Könönen E, Gursoy M, Gursoy UK. Periodontitis: a multifaceted disease of tooth supporting tissues. *J Clin Med*. 2019;8(8):1135. doi:10.3390/jcm8081135
3. Ma YF, Yan XZ. Periodontal guided tissue regeneration membranes: limitations and possible solutions for the bottleneck analysis. *Tissue Eng Part B Rev*. 2023;29(5):532-544. doi:10.1089/ten.TEB.2023.0040
4. Mirzaeei S, Ezzati A, Mehrandish S, Asare-Addo K, Nokhodchi A. An overview of guided tissue regeneration (GTR) systems designed and developed as drug carriers for management of periodontitis. *J Drug Deliv Sci*. 2022;71:103341. doi:10.1016/j.jddst.2022.103341
5. Fan L, Wu D. Enamel matrix derivatives for periodontal regeneration: recent developments and future perspectives. *J Health Eng*. 2022;2022:8661690. doi:10.1155/2022/8661690 Retraction in: J Health Eng. 2023:24; 2023:9867516.

6. Takeda K, Mizutani K, Matsuura T, et al. Periodontal regenerative effect of enamel matrix derivative in diabetes. *PLoS One*. 2018;13(11):e0207201. doi:10.1371/journal.pone.0207201

7. Wei L, Teng F, Deng L, et al. Periodontal regeneration using bone morphogenetic protein 2 incorporated biomimetic calcium phosphate in conjunction with barrier membrane: a preclinical study in dogs. *J Clin Periodontol*. 2019;46:1254-1263. doi:10.1111/jcpe.13195

8. Meghil MM, Mandil O, Nevins M, Saleh MHA, Wang HL. Histologic evidence of Oral and periodontal regeneration using recombinant human platelet-derived growth factor. *Medicina*. 2023;59:676. doi:10.3390/medicina59040676

9. Nevins M, Kao RT, McGuire MK, et al. Platelet-derived growth factor promotes periodontal regeneration in localized osseous defects: 36-month extension results from a randomized, controlled, double-masked clinical trial. *J Periodontol*. 2013;84(4):456-464. doi:10.1902/jop.2012.120141

10. Cho MI, Lin WL, Genco RJ. Platelet-derived growth factor-modulated guided tissue regenerative therapy. *J Periodontol*. 1995;66(6):522-530. doi:10.1902/jop.1995.66.6.522

11. Lynch SE, Williams RC, Polson AM, et al. A combination of platelet-derived and insulin-like growth factors enhances periodontal regeneration. *J Clin Periodontol*. 1989;16(8):545-548. doi:10.1111/j.1600-051x.1989.tb02334.x

12. Ripamonti U, Petit JC, Teare J. Cementogenesis and the induction of periodontal tissue regeneration by the osteogenic proteins of the transforming growth factor-beta superfamily. *J Periodontal Res*. 2009;44(2):141-152. doi:10.1111/j.1600-0765.2008.01158.x

13. Iviglia G, Kargozar S, Baino F. Biomaterials, current strategies, and novel Nano-technological approaches for periodontal regeneration. *J Funct Biomater*. 2019;10(1):3. doi:10.3390/jfb10010003

14. Ouchi T, Nakagawa T. Mesenchymal stem cell-based tissue regeneration therapies for periodontitis. *Regen Ther*. 2020;14:72-78. doi:10.1016/j.reth.2019.12.011

15. Birkedal-Hansen H, Butler WT, Taylor RE. Proteins of the periodontium. Characterization of the insoluble collagens of bovine dental cementum. *Calcif Tissue Res*. 1977;23(1):39-44. doi:10.1007/BF02012764

16. McKee MD, Zalzal S, Nanci A. Extracellular matrix in tooth cementum and mantle dentin: localization of osteopontin and other noncollagenous proteins, plasma proteins, and glycoconjugates by electron microscopy. *Anat Rec*. 1996;245(2):293-312. doi:10.1002/(SICI)1097-0185(199606)245:2<293::AID-AR13>3.0.CO;2-K

17. Groeneveld MC, Everts V, Beertsen W. Alkaline phosphatase activity in the periodontal ligament and gingiva of the rat molar: its relation to cementum formation. *J Dent Res*. 1995;74(7):1374-1381. doi:10.1177/00220345950740070901

18. Matsuura M, Herr Y, Han KY, Lin WL, Genco RJ, Cho MI. Immunohistochemical expression of extracellular matrix components of normal and healing periodontal tissues in the beagle dog. *J Periodontol*. 1995;66(7):579-593. doi:10.1902/jop.1995.66.7.579

19. Alvarez-Pérez MA, Narayanan S, Zeichner-David M, Rodríguez Carmona B, Arzate H. Molecular cloning, expression and immunolocalization of a novel human cementum-derived protein (CP-23). *Bone*. 2006;38(3):409-419. doi:10.1016/j.bone.2005.09.009

20. Valdés De Hoyos A, Hoz-Rodríguez L, Arzate H, Narayanan AS. Isolation of protein-tyrosine phosphatase-like member-a variant from cementum. *J Dent Res*. 2012;91(2):203-209. doi:10.1177/0022034511428155

21. Villarreal-Ramírez E, Moreno A, Mas-Oliva J, et al. Characterization of recombinant human cementum protein 1 (hrCEMP1): primary role in biomineralization. *Biochem Biophys Res Commun*. 2009;384(1):49-54. doi:10.1016/j.bbrc.2009.04.072

22. Montoya G, Correa R, Arenas J, et al. Cementum protein 1-derived peptide (CEMP 1-p1) modulates hydroxyapatite crystal formation in vitro. *J Pept Sci*. 2019;25(10):e3211. doi:10.1002/psc.3211

23. Montoya G, Arenas J, Romo E, et al. Human recombinant cementum attachment protein (hrPTPLa/CAP) promotes hydroxyapatite crystal formation in vitro and bone healing in vivo. *Bone*. 2014;69:154-164. doi:10.1016/j.bone.2014.09.014

24. Serrano J, Romo E, Bermúdez M, et al. Bone regeneration in rat cranium critical-size defects induced by cementum protein 1 (CEMP1). *PLoS One*. 2013;8(11):e78807. doi:10.1371/journal.pone.0078807

25. Ureiro-Cueto G, Rodil SE, Santana-Vázquez M, Hoz-Rodriguez L, Arzate H, Montoya-Ayala G. Characterization of aTiO$_2$ surfaces functionalized with CAP-p15 peptide. *J Biomed Mater Res A*. 2024;112:1399-1411. doi:10.1002/jbm.a.37676

26. Campos MN, Giraldo EL, Del Rio PF, Fernández-Velasco DA, Arzate H, Romo-Arévalo E. Solution NMR structure of cementum protein 1 derived peptide (CEMP1-p1) and its role in the mineralization process. *J Pept Sci*. 2023;29(10):e3494. doi:10.1002/psc.3494

27. Komaki M, Iwasaki K, Arzate H, Narayanan AS, Izumi Y, Morita I. Cementum protein 1 (CEMP1) induces a cementoblastic phenotype and reduces osteoblastic differentiation in periodontal ligament cells. *J Cell Physiol*. 2012;227(2):649-657. doi:10.1002/jcp.22770

28. Lowry OH, Roberts NR, Wu MI, Hixon WS, Crawford EJ. The quantitative histochemistry of brain. II. Enzyme measurements. *J Biol Chem*. 1954;207(1):19-37.

29. Bradford MM. A rapid and sensitive method for the quantitation of microgram quantities of protein utilizing the principle of protein-dye binding. *Anal Biochem*. 1976;72:248-254. doi:10.1006/abio.1976.9999

30. Ruan Q, Zhang Y, Yang X, Nutt S, Moradian-Oldak J. An amelogenin–chitosan matrix promotes assembly of an enamel-like layer with a dense interface. *Acta Biomater*. 2013;9(7):7289-7297. doi:10.1016/j.actbio.2013.04.004

31. Beertsen W, Van den Bos T. Alkaline phosphatase induces the deposition of calcified layers in relation to dentin: an in vitro study to mimic the formation of afibrillar acellular cementum. *J Dent Res*. 1991;70(3):176-181. doi:10.1177/00220345910700030401

32. Hartgerink JD, Beniash E, Stupp SI. Self-assembly and mineralization of peptide-amphiphile nanofibers. *Science*. 2001;294:1684-1688.

33. Chen JK, Shapiro HS, Wrana JL, Reimers S, Heersche JNM, Sodek J. Localization of bone sialoprotein (BSP) expression to sites of mineralized tissue formation in fetal rat tissues by in situ hybridization. *Matrix*. 1991;11:133-143. doi:10.1016/s0934-8832(11)80217-9Hj

34. Chen J, Shapiro HS, Sodek J. Development expression of bone sialoprotein mRNA in rat mineralized connective tissues. *J Bone Miner Res*. 1992;7:987-997. doi:10.1002/jbmr.5650070816

35. Ganss B, Kim RH, Sodek J. Bone sialoprotein. *Crit Rev Oral Biol Med*. 1999;10(1):79-98. doi:10.1177/10454411990100010401

36. Fisher LW, Torchia DA, Fohr B, Young MF, Fedarko NS. Flexible structures of SIBLING proteins, bone sialoprotein, and osteopontin. *Biochem Biophys Res Commun*. 2001;280:460-465. doi:10.1006/bbrc.2000.4146

37. Konka J, Espanol M, Bosch BM, de Oliveira E, Ginebra MP. Maturation of biomimetic hydroxyapatite in physiological fluids: a physicochemical and proteomic study. *Mater Today Bio*. 2021;12:100137. doi:10.1016/j.mtbio.2021.100137

38. El-Sayed B, Davies RPW, El-Zehery RR, et al. An *in-vivo* intraoral defect model for assessing the use of P$_{11}$-4 self-assembling peptide in periodontal regeneration. *Front Bioeng Biotechnol*. 2020;8:559494. doi:10.3389/fbioe.2020.559494

39. Gungormus M, Oren E, Horst J, et al. Cementomimetics-constructing a cementum-like biomineralized microlayer *via* amelogenin-derived peptides. *Int J Oral Sci*. 2012;4:69-77. doi:10.1038/ijos.2012.40

40. Chiu HC, Chiang CY, Tu HP, Wikesjö UM, Susin C, Fu E. Effects of bone morphogenetic protein-6 on periodontal wound healing/regeneration in supraalveolar periodontal defects in dogs. *J Clin Periodontol*. 2013;40(6):624-630. doi:10.1111/jcpe.12075

41. Yukna R, Salinas TJ, Carr RF. Periodontal regeneration following use of ABM/P-1 5: a case report. *Int J Periodont & Rest Dent*. 2002;22(2):146-155.

42. Yamashita M, Lazarov M, Jones AA, Mealey BL, Mellonig JT, Cochran DL. Periodontal regeneration using an anabolic peptide with two carriers in baboons. *J Periodontol*. 2010;81(5):727-736. doi:10.1902/jop.2010.090224

43. Kémoun P, Laurencin-Dalicieux S, Rue J, et al. Human dental follicle cells acquire cementoblast features under stimulation by BMP-2/−7 and enamel matrix derivatives (EMD) in vitro. *Cell Tissue Res*. 2007;329(2):283-294. doi:10.1007/s00441-007-0397-3

44. Hoz L, López S, Zeichner-David M, Arzate H. Regeneration of rat periodontium by cementum protein 1-derived peptide. *J Periodontal Res*. 2021;56(6):1223-1232. doi:10.1111/jre.12921

SUPPORTING INFORMATION

Additional supporting information can be found online in the Supporting Information section at the end of this article.